Virology 456-457 (2014) 121–130

Contents lists available at ScienceDirect

Virology

journal homepage: www.elsevier.com/locate/yviro

Effect of specific amino acid substitutions in the putative fusion peptide of structural glycoprotein E2 on Classical Swine Fever Virus replication

I.J. Fernández-Sainz [a], E. Largo [b], D.P. Gladue [a], P. Fletcher [a], V. O'Donnell [a,c], L.G. Holinka [a], L.B. Carey [d], X. Lu [c], J.L. Nieva [b], M.V. Borca [a,*]

[a] Plum Island Animal Disease Center, ARS, USDA, USA
[b] Biophysics Unit (CSIC-UPV/EHU), Department of Biochemistry and Molecular Biology, University of the Basque Country (UPV/EHU), P.O. Box 644, 48080 Bilbao, Spain
[c] Plum Island Animal Disease Center, DHS, Greenport, NY 11944, USA
[d] Department of Experimental and Health Sciences, Universitat Pompeu Fabra (UPF), E-08003 Barcelona, Spain

ARTICLE INFO

Article history:
Received 6 February 2014
Returned to author for revisions
25 February 2014
Accepted 4 March 2014
Available online 4 April 2014

Keywords:
Fusion peptide
Classical Swine Fever Virus
CSFV
Classical swine fever
Pestivirus

ABSTRACT

E2, along with E^{rns} and E1, is an envelope glycoprotein of Classical Swine Fever Virus (CSFV). E2 is involved in several virus functions: cell attachment, host range susceptibility and virulence in natural hosts. Here we evaluate the role of a specific E2 region, ^{818}CPIGWTGVIEC^{828}, containing a putative fusion peptide (FP) sequence. Reverse genetics utilizing a full-length infectious clone of the highly virulent CSFV strain Brescia (BICv) was used to evaluate how individual amino acid substitutions within this region of E2 may affect replication of BICv. A synthetic peptide representing the complete E2 FP amino acid sequence adopted a β-type extended conformation in membrane mimetics, penetrated into model membranes, and perturbed lipid bilayer integrity *in vitro*. Similar peptides harboring amino acid substitutions adopted comparable conformations but exhibited different membrane activities. Therefore, a preliminary characterization of the putative FP ^{818}CPIGWTGVIEC^{828} indicates a membrane fusion activity and a critical role in virus replication.

Published by Elsevier Inc.

Introduction

Classical swine fever (CSF) is a highly contagious disease of swine caused by CSF virus (CSFV), a small enveloped virus with a positive-sense, single-strand RNA genome. CSFV is classified as a member of the pestivirus genus within the *Flaviviridae* family along with other viruses of economic importance, bovine viral diarrhea virus (BVDV) and border disease virus (BDV) (Becher et al., 2003). The approximately 12.5-kb CSFV genome contains a single open reading frame that encodes a polyprotein composed of 3898 amino acids that ultimately yields up to 12 final cleavage products (NH2-Npro-C-Erns-E1-E2-p7-NS2-NS3-NS4A-NS4B-NS5A-NS5B-COOH) through co- and post-translational processing of the polyprotein by cellular and viral proteases (Rice, 1996).

Structural components of the virion include the capsid (C) protein and glycoproteins: E^{rns}, E1 and E2. E^{rns}, a secreted protein that demonstrates RNAse activity and is loosely associated with the viral envelope (Thiel et al., 1991; Weiland et al., 1990; Weiland et al., 1999), does not have a hydrophobic transmembrane anchor domain. E^{rns} does, however, possess a C-terminal charged amphipathic segment that can mediate translocation of E^{rns} across bilayer membranes (Langedijk, 2002). E1 and E2 are transmembrane proteins with an N-terminal ectodomain and a C-terminal hydrophobic anchor (Thiel et al., 1991). E2 is considered essential for CSFV replication, as virus mutants containing partial or complete deletions of the E2 gene are nonviable (van Gennip et al., 2002). E2 has been implicated, along with E^{rns} (Hulst and Moormann, 1997) and E1 (Wang et al., 2004), in viral adsorption to host cells (Liang et al., 2003; van Gennip et al., 2000). Modifications introduced into this glycoprotein appear to have an important effect on CSFV virulence (Risatti et al., 2005, 2006, 2007a, 2007b; Van Gennip et al., 2004).

Using proteomic computational analysis, E2 has been characterized as a truncated class II fusion protein (Garry and Dash, 2003). Although the overall structures of class I and II fusion proteins are distinct, they may share structural/functional characteristics in the parts of the molecules that interact with and disrupt bilayer membranes. It is well established that class I fusion proteins have a fusion peptide at the amino terminus of the

* Correspondence to: Plum Island Animal Disease Center, USDA/ARS/NAA, P.O. Box 848, Greenport, NY 11944-0848, USA. Tel.: +1 631 323 3019; fax: +1 631 323 3006.
E-mail address: manuel.borca@ars.usda.gov (M.V. Borca).

http://dx.doi.org/10.1016/j.virol.2014.03.005
0042-6822/Published by Elsevier Inc.

molecule, or close to it, that is critical for fusion (Gallaher, 1987, 1996; Gallaher et al., 1989, 2001). Class II fusion proteins have an internal FP that is located after secondary structural folding at distal locations from the transmembrane anchor (Kuhn et al., 2002; Lescar et al., 2001; Rey et al., 1995). Garry and Dash described a putative FP located between amino acid residues 818–828 of CSFV E2. This putative FP contains a consensus sequence with aromatic and hydrophobic residues located between two cysteine residues. In addition, the FP is flanked by β sheets in class II fusion proteins. The cysteine residues as well as the sequences in between are highly conserved among pestiviruses, as is true of class I and II FPs from other enveloped RNA viruses (Garry and Dash, 2003). Recently the E2 protein of BVDV has been crystallized, revealing a three β-domain structure (El Omari et al., 2013). The putative FP appears to be partially accessible on the surface of the protein. However, it does not form a canonical fusion loop as those found in Class II proteins, which suggests that other mechanisms-structures might operate in pestivirus fusion.

Here we evaluate the role of a specific E2 region, ^{818}CPIGWTGVIEC^{828}, containing a putative FP sequence. Reverse genetics utilizing a full-length infectious clone of the highly virulent strain Brescia (BICv) was used to evaluate the role of individual as well as combined amino acid substitutions in the replication of BICv. Only double C818S/C828S or triple P819S/I820S/W822S substitutions resulted in replication-deficient viruses. Furthermore, we sought to establish a correlation between the functional effects induced by the amino acid substitutions and the capacity of synthetic FPs for inserting into membranes and breach the permeability barrier. At the outset we confirmed the retention of β-type extended conformations in membrane mimics for the native sequence and its variants harboring the double C818S/C828S or triple P819S/I820S/W822S substitutions. Our data indicate that amino acid substitutions primarily affect the degree of FP penetration into the lipid bilayer, the triple substitution resulting in shallower insertion and reduced membrane activity. All in all, our results suggest that the putative FP ^{818}CPIGWTGVIEC^{828} is involved in membrane fusion activity and plays a critical role in virus replication.

Results

Location of the putative fusion peptide in the CSFV E2 protein

The putative E2 FP is formed by eleven amino acids situated between positions 818 and 828 of the CSFV polypeptide. Comparison of its amino acid sequence among different CSFV isolates reveals 100% identity among isolates (Fig. 1). Compared to other pestiviruses the amino acid identity ranges between 45 and 72% similar to BVDV isolates with substitutions mostly occurring at positions 820 and 825–827, 63–72% similar to BDV isolates with amino acid substitutions at positions 820, 822, 824, 825, and 81% similar to pestivirus giraffe-1 with substitutions at 823–825. This high degree of conservation within each of the pestivirus subgroups, compared to the differences between the subgroups, suggests the putative FP sequence may be involved in an important viral function such as virus tropism.

Development of CSFV infectious clones harboring amino acid substitutions in the FP sequence

To evaluate the role of the putative FP in the *in vitro* and *in vivo* replication of CSFV as well as in the production of disease in swine, a series of recombinant CSF viruses containing amino acid substitutions in the FP area were designed using the cDNA infectious clone of the Brescia strain (BICv) as a template. A total of eight cDNA constructs containing the amino acid substitutions described in Table 1 were constructed.

Infectious RNA was *in vitro* transcribed from each mutated full-length cDNA and used to transfect SK6 cells. Infectious virus containing individual substitutions of C818S, C828S, P819S, I820T, W822S or double substitution V825T/I826T was rescued from transfected cells by day 4 post-transfection. Partial nucleotide sequence of the rescued mutant E2 viruses was performed to ensure the presence of the predicted mutations (data not shown).

Conversely, in three independent transfection events, constructs harboring a double, C818S/C828S, or triple, P819S/I820S/W822S, substitutions were unvaryingly negative in terms of recovering infectious particles (data not shown). Immunohistochemistry analysis of transfected cell monolayers showed that cells transfected with either construct C818S/C828S or P819S/I820S/W822S expressed E2 (Fig. 2A) although at a decreased level when compared to those found in cells transfected with the constructs producing viable virus particles.

Thus, to determine if a gross defect in glycosylation of truncated expression was at the origin of the lethal phenotype, the expression of E2 glycoprotein in cells transfected with either C818S/C828S or P819S/I820S/W822S was additionally analyzed by Western blot. Cell extracts transfected with either of these two constructs demonstrated significant levels of E2 expression with a product showing an electrophoretic mobility similar to that observed with cell extracts transfected with an IC encoding for the parental Brescia virus (Fig. 2B). These results suggest that the double and triple substitution constructs produced a lethal replication virus phenotype, even though there is efficient expression of an apparently intact E2 product.

Replication of the CSFV FP mutants in vitro

in vitro replication characteristics of the FP E2 mutant viruses containing individual (C818S, C828S, P819S, I820T, W822S) or double substitutions (V825T/I826T) relative to parental BICv were evaluated in a single-step growth curve. Primary swine macrophage cell cultures were infected at a MOI of 0.01 $TCID_{50}$ per cell. Viruses were adsorbed for 1 h (time zero), and samples were collected at 72 h post-infection and titrated in SK6 cell cultures. All mutant viruses exhibited growth kinetics almost undistinguishable from that of the parental BICv (Fig. 3A). Additionally, when the FP E2 mutant viruses' plaque sizes were compared using SK6 cells, all mutants exhibited a plaque size similar to that of the parental BICv (Fig. 3B). Therefore, individual substitutions of most of the residues forming the putative FP do not significantly affect the ability of the virus to replicate in cell cultures.

Virulence of CSFV FP mutants in vivo

To examine whether alterations of different residues included in the putative E2 FP affect virulence, different groups of pigs were intranasally inoculated with approximately 10^5 $TCID_{50}$ of each of the E2 FP mutant viruses (C818S, C828S, P819S, I820T, W822S, V825T/I826T) and monitored for clinical disease, evaluated relative to parental BICv. All animals infected with BICv presented clinical signs of CSF starting 3–4 days post-infection (DPI), developing classic symptoms of the disease and dying around 7–8 DPI (Table 2). Total white blood cells, lymphocytes and platelet counts dropped by 4–6 DPI in animals inoculated with BICv and continued declining until death (data not shown). All mutant viruses presented a virulence phenotype almost indistinguishable from that of the parental BICv (Table 2). All animals infected with these viruses presented clinical signs of CSF starting at 3–5 DPI, with clinical presentation and severity similar to those observed in

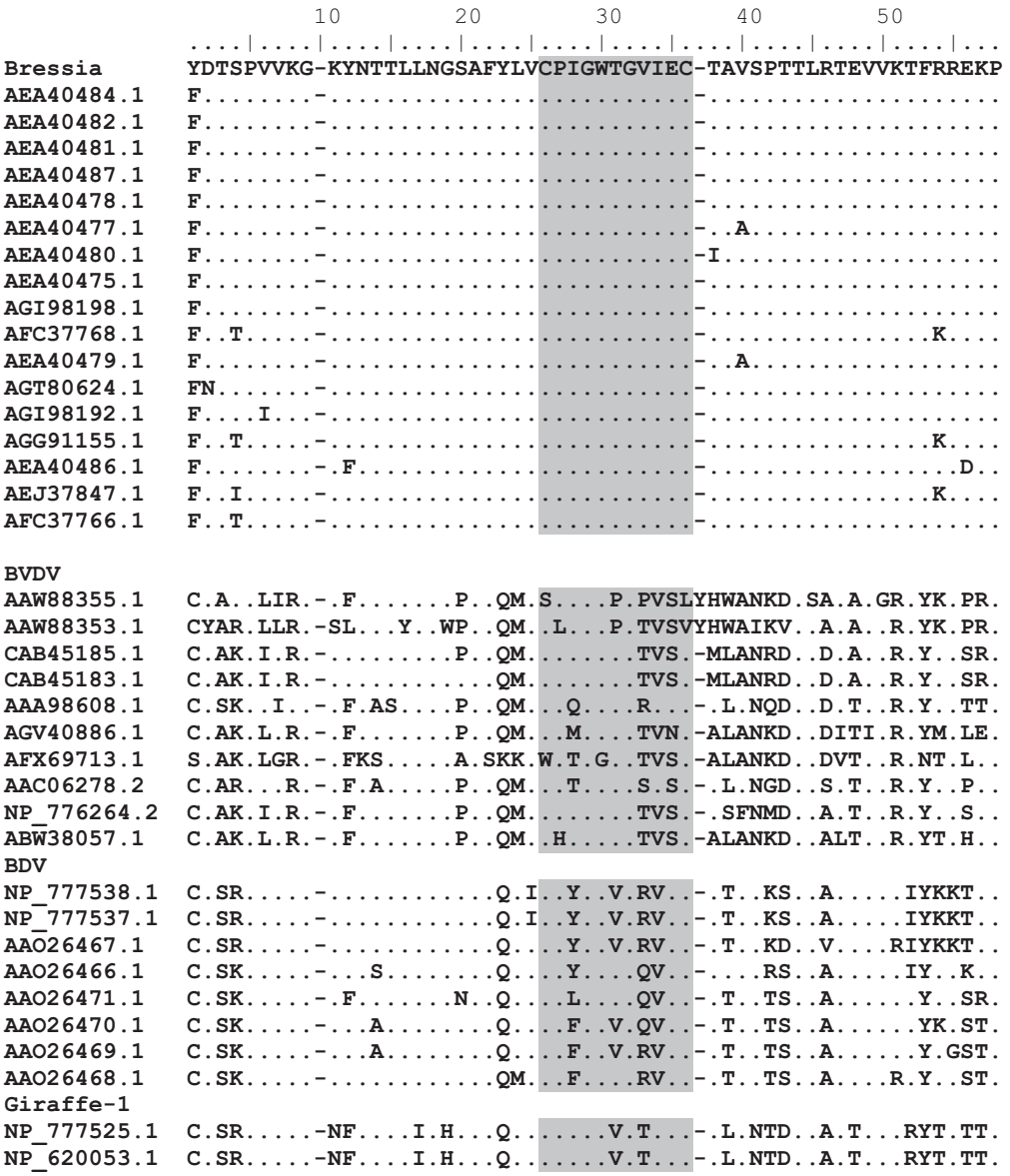

Fig. 1. Sequence alignment to show putative FP sequences (highlighted) of E2 from different Pestiviruses (CSF, BVD, BD and Giraffe-1). Partial amino acid sequence surrounding polypeptide residues 818–828 are presented.

Table 1
Nucleotide sequence of primers used for the production of E2FP recombinant viruses (only forward primers are presented).

Mutant name	Forward primer sequence
C818S	5′ GGTAGTGCATTCTACCTAGTTTGCCCAATAGGGTGGACGGGTGTT 3′
C828S	5′ GGGTGGACGGGTGTTATAGAGTGCACGGCAGTGAGCCCGACAACT 3′
C818S/C828S	[a]
P819S	5′ AGTGCATTCTACCTAGTTTGCTCAATAGGGTGGACGGGTGTTATA 3′
I820T	5′ GCATTCTACCTAGTTTGCCCAACAGGGTGGACGGGTGTTATAGAG 3′
W822S	5′ TACCTAGTTTGCCCAATAGGGTCGACGGGTGTTATAGAGTGCACG 3′
P819S/I820S/W822S	5′ GCATTCTACCTAGTTTGCTCAACAGGGTCGACGGGTGTTATAGAGTGC 3′
V825T/I826T	5′ TGCCCAATAGGGTGGACGGGTGATACAGAGTGCACGGCAGTGAGCCCG 3′

[a] Primers C818S and C828S were consecutively used to create mutant C818S/C828S.

animals inoculated with BICv. White blood cells, lymphocytes and platelet counts dropped by 4 DPI and continued declining until death (data not shown) at 6–9 DPI.

Viremia in animals inoculated with E2 FP mutants in general accompanied the evolution of the clinical disease (data not shown), exhibiting viremia kinetics almost undistinguishable from that induced by parental BIC virus, presenting high titers that remained until death of the animal.

Therefore, with the exception of the lethal substitutions C818S/C828S or P819S/I820S/W822S, substitutions of any of the other

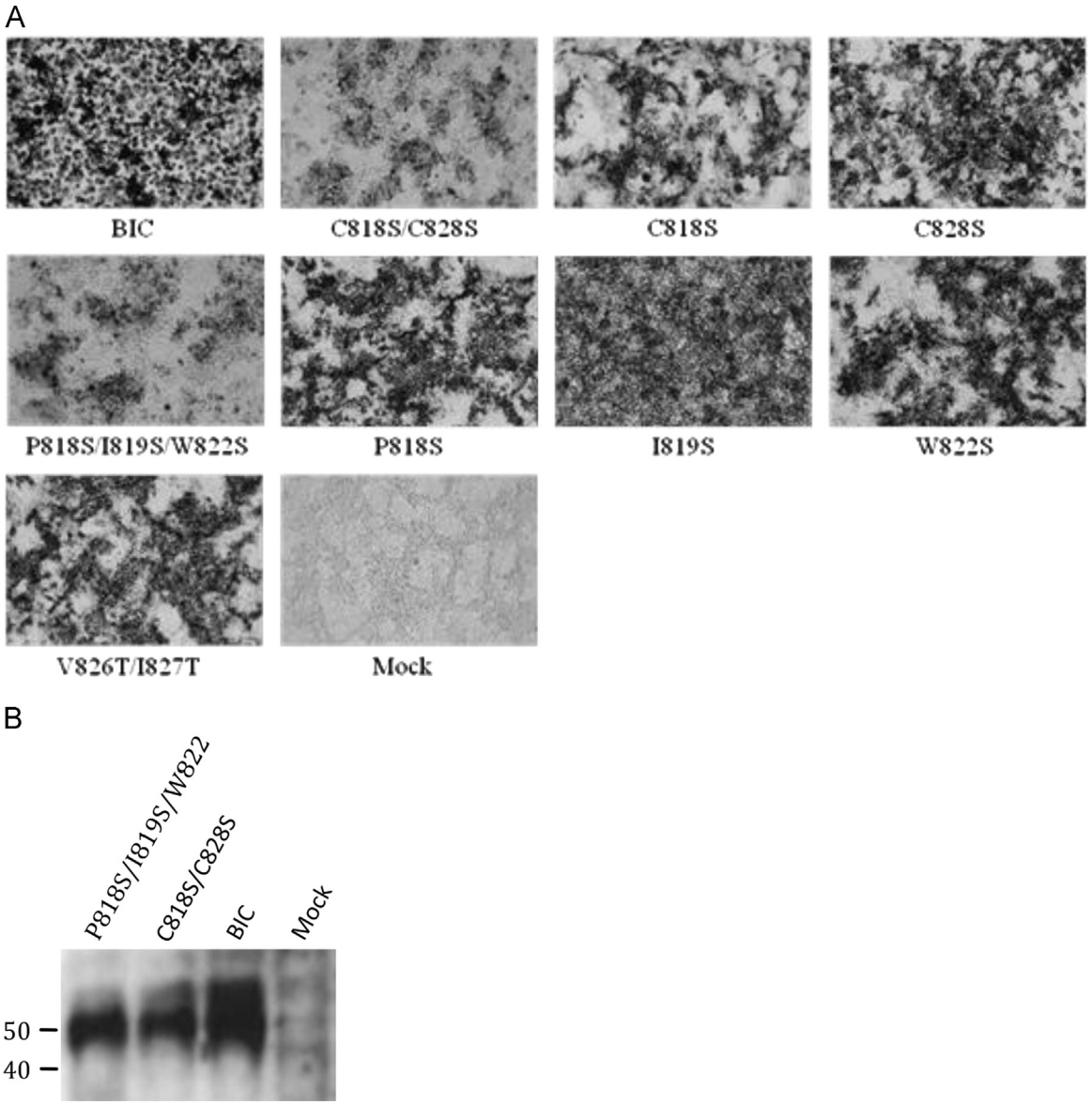

Fig. 2. Expression of E2 glycoprotein in SK6 cells transfected with the indicated constructs (detection was performed using anti-E2 mAb WH303) by (A) immunocytochemistry, and (B) Western blot.

residues under study within the FP area do not significantly affect virus growth in cell culture or pathogenesis in swine.

Evaluation in vitro of the putative fusion peptide in terms of structure and membrane interaction

To determine the effect of the amino acid substitutions on the adopted conformations and the interactions with membranes, three FP variant peptides were synthesized and comparatively analyzed. One of the synthetic peptides represents the native sequence of the E2 FP (designated as WT) while the other two harbor a double (C818S/C828S) or a triple substitution (P819S/I820S/W822S) and were designated as mut-1 and mut-2, respectively (Fig. 4A). All three sequences were flanked by additional lysine residues to confer solubility, and tagged at the N-terminus with the NBD fluorescent probe for assessment of interactions with lipid bilayers. The secondary structures adopted by these synthetic peptides are displayed in Fig. 4B. Circular dichroism measurements disclosed comparable amounts of β-type extended structures that were predominant for the three variants, and overall retained in the membrane-mimicking environments provided by SDS and DPC micelles. Thus, the amino acid substitutions did not seem to affect the secondary structure of the E2 FP, which otherwise performed comparably in solution and the low-polarity membrane environment.

Membrane interactions of WT, mut-1 and mut-2 variants were next assessed in lipid monolayer and unilamellar vesicle models (Fig. 5). The three sequences were first compared in the lipid monolayer system, which allows monitoring peptide penetration into membranes as an increase of the monolayer lateral pressure (see Largo et al. 2014 for a description of the system). The system also allows adjustment of the initial lateral pressure (π_0). Thus, the FP capacity of raising the monolayer lateral pressure upon injection at high $\pi_0 - s$ (*i.e.*, with tightly packed phospholipids) will correlate with its capacity for inserting into the viral target membrane (Nieva and Agirre, 2003; Rafalski et al., 1990). Penetration levels of the synthetic FPs depending on π_0 are shown in Fig. 5A. The monolayer exclusion pressures, π_{ex}, or the maximum initial lateral pressures at which membrane-association was accompanied by peptide integration into the monolayer, were

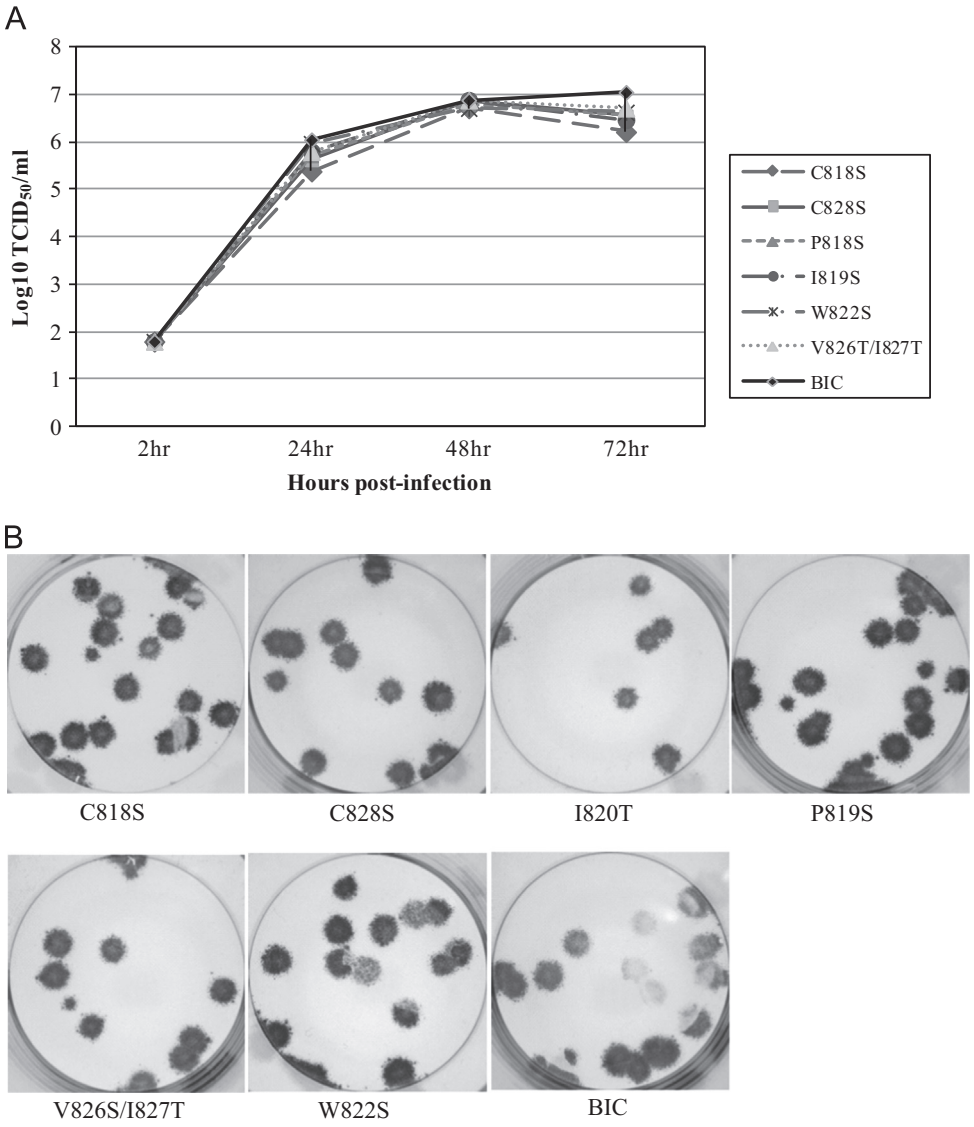

Fig. 3. *in vitro* growth characteristics of FP mutants and parental BICv. **(A)** Primary swine macrophage cell cultures were infected (MOI=0.01) with each of the FP virus mutants or BICv and virus yield titrated at times post-infection in SK6 cells. Data represent means and standard deviations from two independent experiments. Sensitivity of virus detection: ≥ 1.8 TCID50/ml. (B) Plaque formation of the FP virus mutants and BICv. SK6 monolayers were infected, overlaid with 0.5% agarose and incubated at 37 °C for 3 days. Plates were fixed with 50% (vol/vol) ethanol-acetone and stained by immunohistochemistry with mAb WH303.

Table 2
Swine survival and fever response following infection with E2FP mutants and parental BICv.

Virus	No. of survivors/ total no.	Mean time to death (days ± SD)	Fever	
			No. of days to onset (days ± SD)	Duration (days ± SD)
BIC	0/4	7.75 (1.5)	3.75 (0.9)	5 (1.4)
C818S	0/4	7.25 (0.9)	4 (0.0)	4.25 (0.9)
C828S	0/4	6.75 (2.1)	4 (0.0)	3.75 (0.9)
P819S	0/4	7.75 (0.5)	5 (1.1)	4.75 (1.7)
W822S	0/4	9.5 (3)	5.5 (2.3)	4.75 (1.7)
V825T/ I826T	0/4	9.5 (2.3)	3.5 (1)	7 (2.1)
I820T	0/4	8.5 (2.1)	3.5 (0.7)	6 (1.4)

comparable for WT and mut-1, and consistent with their penetration into membranes with the lipid packing density existing at the target cell membrane ($\pi_c \geq 30$ mN/m, (Marsh, 2007). In contrast, the mut-2 variant was unable to efficiently penetrate into monolayers compressed to those levels.

To determine degrees of association with lipid bilayers, we next compared partitioning of the three sequences into vesicles by monitoring changes in the emitted NBD-fluorescence (Fig. 5B). The partitioning coefficients, estimated upon titrating the peptides with increasing quantities of vesicles, were all in the range of 10^5, therefore denoting comparable degrees of association for the three variants. However, NBD intensity increased by a factor of 10 in the case of the mut-1 peptide, while this factor was reduced to 3 for the mut-2 peptide. The higher increase in emission intensity was consistent with deeper penetration of the fluorophore into the hydrocarbon core of the lipid bilayer in the former case. The WT NBD emission increased by a factor of 5, consistent with an intermediate level of insertion. In summary, lipid monolayer and NBD-fluorescence results suggest that the triple substitution interferes with FP penetration into the target membrane, while replacing the CC residues results in deeper insertion into the low-polarity region.

Finally, results displayed in Fig. 5C revealed that WT inserted into membranes was capable of perturbing the lipid bilayer

A

WT: NBD-KKFYLVCPIGWTGVIECTAVSKK
mut-1: NBD-KKFYLV**S**PIGWTGVIE**S**TAVSKK
mut-2: NBD-KKFYLVC**ST**G**S**TGVIECTAVSKK

B

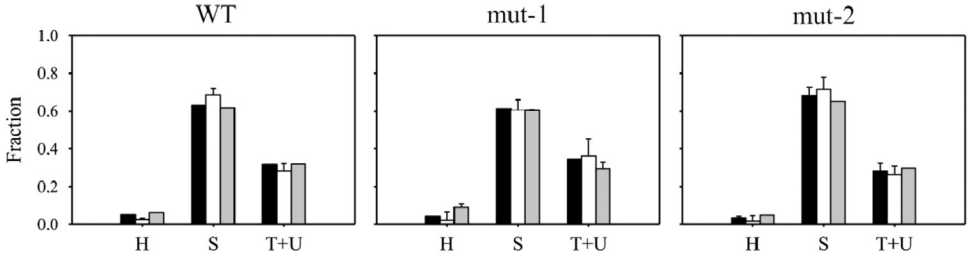

Fig. 4. Designation and structure of E2 FP-derived synthetic peptides. (A) Designation and sequences of the peptides used in this study. Substituted residues are indicated in bold. (B) Secondary structures. The structural components were calculated for the CD spectra obtained in buffer (black bars), or in the presence of 100 mM DPC (white bars) or 100 mM SDS (gray bars). Means ± SD for the fraction values estimated with CONTIN-LL, CDSSTR and SELCON3 programs are plotted for the peptides as indicated in the panels. H, helix; S, strand; T+U, turns+unordered.

architecture more efficiently than the mutant-representing peptides. In these assays the integrity of the POPG membrane was monitored using the ANTS/DPX assay (Nieva et al., 1994; Rafalski et al., 1990). A peptide-to-lipid ratio of 1:700 was required to induce 50% of vesicle permeabilization by WT, whereas the ratio increased to 1:300 for mut-1 and this level of permeabilization was barely attained with the highest dose of mut-2 tested (1:100). Thus, for comparable amounts of peptide associated with the membrane, the WT sequence was more efficient than the mutants at destabilizing the integrity of the vesicles.

Discussion

This report attempted to characterize the role of the putative FP comprising the amino acid residues ^{818}CPIGWTGVIEC^{828} of glycoprotein E2 in CSFV. Reverse genetics and an *in vitro* artificial membrane assays were used to assess the role of individual residues within the E2 FP in the process of virus replication and membrane insertion. Double (C818S/C828S) or triple (P819S/I820S/W822S) residue substitutions completely abrogate virus replication, additionally, the triple substitution led to a decreased capacity for membrane insertion.

The characterization of the structure and membrane interactions of synthetic peptides representing the double and triple substitutions in the FP indicated that the conformations adopted by the WT and mutated peptides were compatible with the extended β-type structure of the FP. Such structures were not significantly altered in the presence of membrane mimetics, indicating the amino acid substitutions did not affect the overall conformation adopted by the FP in solution or the low-polarity membrane-like environment. In contrast, the three peptides displayed different patterns of interactions with membrane models. The ability of synthetic peptides and their mutant variants to penetrate into POPG monolayers was earlier described for the HIV-1 FP (Nieva et al., 1994; Rafalski et al., 1990). Those studies demonstrated that a polar substitution that inactivated the fusion glycoprotein also interfered with the penetration of the FP into the POPG monolayer. In our experiments, the triple substitution (P819S/I820S/W822S) had a comparable blocking effect on the ability of the E2 FP. This mutant associated with POPG vesicles as efficiently as WT and double substitutions, but induced therein less permeabilization. Thus, we assume that the triple substitution causes a shallower association with the lipid bilayer, a possibility supported by the more polar environment sensed by the NBD fluorescent probe. In this regard, proline and tryptophan residues sustain insertion of the Ebola virus FP as an integral membrane hairpin, and are required for the fusogenic activity of the envelope glycoprotein. Structure and function of the complete internal fusion loop from Ebola virus glycoprotein 2 (Gregory et al., 2011). By analogy, the lack of FP insertion induced by the triple substitution might interfere with E2 fusogenic activity and prevent CSFV infection. By comparison the peptide harboring the double substitution inserted efficiently into monolayers and penetrated deeper into the lipid bilayer surrounding the vesicles (Nieva and Agirre, 2003). In this case it is possible that a di-Sulfide bridge stabilizing a functional integral haipin would be absent in the FP mutant, thereby allowing its deeper insertion but hampering its fusogenic activity. Nonetheless, this mutant was still less efficient than the WT at perturbing the membrane. It is postulated that the membrane restructuring effect will be more potent for peptides inserted at the level of the phospholipid glycerol backbone, than for peptides associated at the level of the headgroups of the phospholipids, or than for those inserted deeper into the acyl-chain region (Nieva and Agirre, 2003). We infer that, compared to the mutant derivatives, the WT peptide attains an intermediate depth of penetration to exert maximal lipid bilayer destabilization effects. This observation would support its role as a membrane-destabilizing anchor during fusion and explain its involvement in viral propagation.

Recently the E2 protein of BVDV has been crystallized, revealing a three domain structure. Domains I and II are similar to Ig-like domains and domain III is a series of three small β-sheet modules; this structure is believed to be similar to CSFV E2 by prediction analysis (Iourin et al., 2013; Li et al., 2013). Using the crystal structure for BVDV-1 E2 at ph 8.0 (pdb:2yq2) (El Omari et al., 2013), the putative FP appears to be partially accessible, however the critical residues P819S/I820S/W822S appear to be mostly internal situated (Fig. 6). In summary, this preliminary characterization of the functionality of the putative FP comprising the amino acid residues ^{818}CPIGWTGVIEC^{828} of glycoprotein E2 in CSFV demonstrated that altering this area although do not significantly alter protein expression, results critical in the process of virus replication and the ability of the protein to be inserted in cell membranes.

Materials and methods

Viruses and cells

Swine kidney cells (SK6) (Terpstra 1990), free of BVDV, were cultured in Dulbecco's minimal essential media (DMEM) (Gibco, Grand Island, NY) with 10% fetal calf serum (FCS) (Atlas Biologicals, Fort Collins, CO). CSFV Brescia strain was propagated in SK6 cells

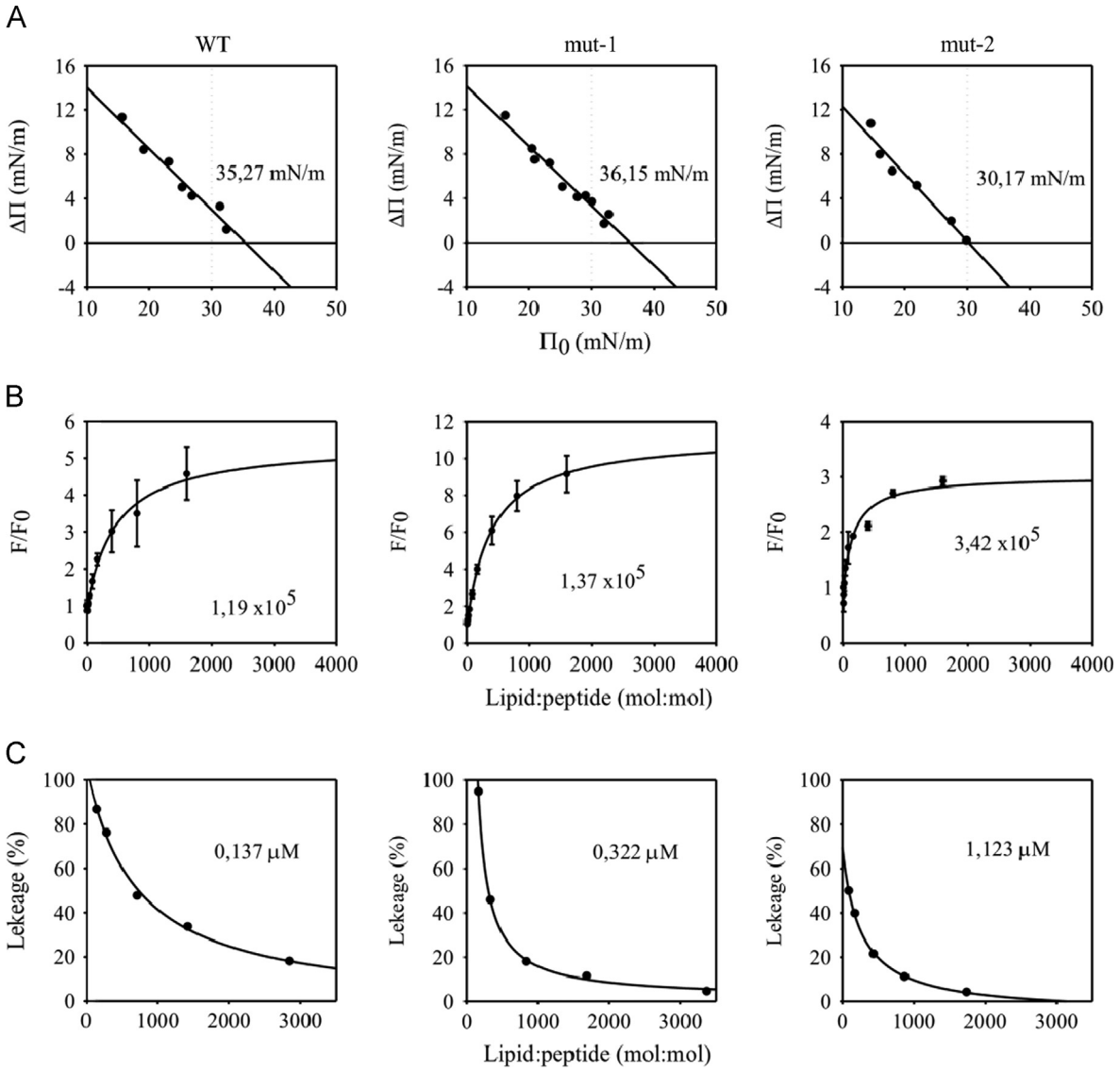

Fig. 5. Interactions with model membranes of E2 FP-derived synthetic peptides. (A) Penetration into POPG monolayers. Maximum increase in surface pressure induced upon injection of 0.4 μM peptide into the subphase was measured as a function of the initial surface pressure of the phospholipid monolayers. Monolayer exclusion pressures are indicated in the panels. The dotted line begins at 30 mN/m. (B) Partitioning curves as estimated from the fractional change in NBD-fluorescence in the presence of increasing amounts of POPG LUV. The solid lines correspond to the best fittings of the experimental values to equation [1]. The estimated K_x values are displayed in the panels. (C) Final extents of ANTS leakage (percentage after 30 min) from POPG LUV as a function of the lipid-to-peptide mole ratio. Lipid concentration (100 μM) was fixed. The amount of peptide bound to membrane was corrected according to the partition coefficients in panel B. EC_{50} values are displayed in the panels.

and was used for the construction of an infectious cDNA clone (Risatti et al., 2005). Growth kinetics was assessed using primary swine macrophage cell cultures prepared as described by Zsak et al. (1996). Titration of CSFV from clinical samples was performed using SK6 cells in 96-well plates (Costar, Cambridge, MA). After 4 days in culture, viral infectivity was assessed using an immunoperoxidase assay utilizing the CSFV monoclonal antibody WH303 (mAb WH303) (Edwards et al., 1991) and the Vectastain ABC kit (Vector Laboratories, Burlingame, CA). Titers were calculated according to the method of Reed and Muench (1938) and expressed as $TCID_{50}$/ml. As performed, test sensitivity was $\geq \log_{10} 1.8$ $TCID_{50}$/ml.

Construction of CSFV mutants

A full-length infectious clone (IC) of the virulent Brescia strain (pBIC) (12) was used as a template to obtain all cDNA IC constructs described in this report. Constructs containing mutations in the FP area were obtained using the QuickChange XL Site-Directed Mutagenesis kit (Stratagene) performed per manufacturer's instructions using full-length pBIC as template and the primers described in Table 1. The product was then digested with Dpn1, leaving only the newly amplified plasmid, transformed into XL10-Gold ultracompetent cells, and grown on Terrific Broth Agar Plates with ampicillin (Teknova). Positive colonies were selected for by sequence analysis of the E2 gene and grown for plasmid purification using a Maxiprep kit (Qiagen Sciences, MD). Each of the IC constructs were completely sequenced to verify that only site-directed mutagenesis-induced changes were present.

in vitro rescue of CSFV Brescia and FP mutants

Full-length genomic clones were linearized with *Srf*I and *in vitro* transcribed using the T7 Megascript system (Ambion, Austin, TX) (Risatti et al., 2005). RNA was precipitated with LiCl and transfected into SK6 cells by electroporation at 500 V, 720 Ω, 100 W with a BTX 630 electroporator (BTX, San Diego, CA). Cells were seeded in 12-well plates and incubated for 4 days at 37 °C

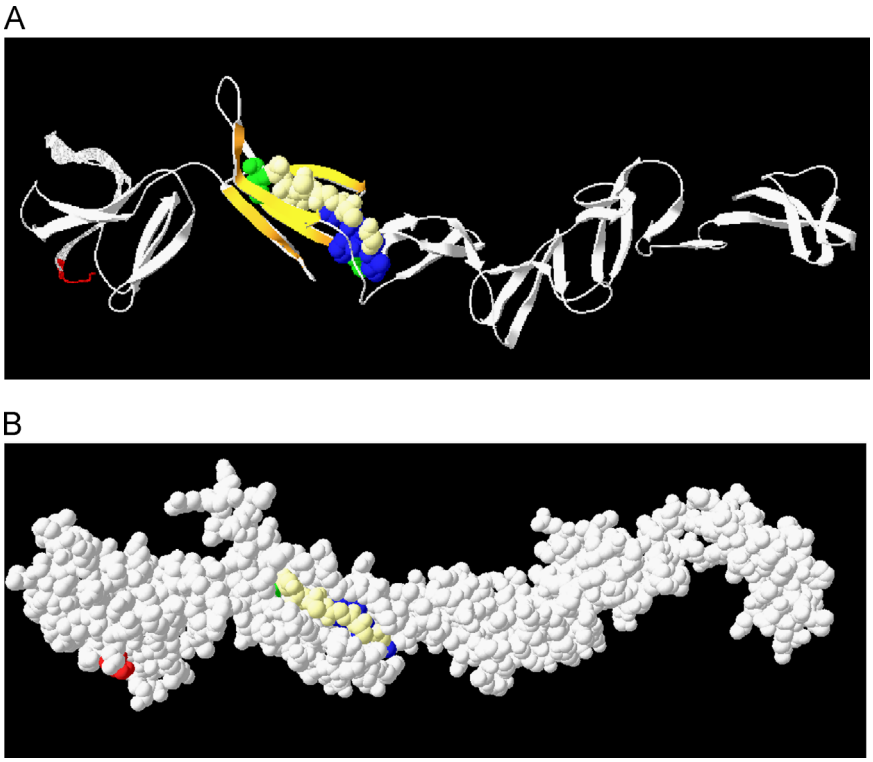

Fig. 6. Location of putative FP into schematic representation of a tridimensional structure of BVDV E2 (El Omari et al., 2013). Critical cystines are presented in green, the PI.W residues in blue, and the remainder of the fusion peptide in yellow. The N-terminus is colored red for orientation. (A) A ribbon model is shown with the fusion peptide colored and the surrounding β-sheets are colored in orange (B) The location of the putative FP it is shown a space filling model.

and 5% CO_2. Virus was detected by immunoperoxidase staining as described above, and stocks of rescued viruses were stored at −70 °C.

DNA sequencing and analysis

Full-length clones and *in vitro* rescued viruses were completely sequenced with CSFV-specific primers by the dideoxynucleotide chain-termination method (Sanger et al., 1977). Viruses recovered from infected animals were sequenced in the region of the genome that contained the desired mutations. Sequencing reactions were prepared with the Dye Terminator Cycle Sequencing Kit (Applied Biosystems, Foster City, CA). Reaction products were sequenced on a PRISM 3730xl automated DNA sequencer (Applied Biosystems). Sequence data was assembled using Sequencher 4.7™ software (Genes Codes Corporation, Ann Arbor, MI). The final DNA consensus sequence represented, on average, a three- or four-fold redundancy at each base position.

Animal infections

Virulence of FP mutant viruses relative to BICv was initially assessed in 10–12 weeks old, forty-pound commercial-breed pigs inoculated intranasally (IN) with 10^5 $TCID_{50}$ of each virus. Pigs were randomly allocated into 7 groups of 4 animals each and were inoculated with a FP virus mutant or BICv. Clinical signs (anorexia, depression, purple skin discoloration, staggering gait, diarrhea and cough) and changes in body temperature were recorded daily throughout the experiment and scored as previously described (Mittelholzer et al., 2000). Blood was collected at times post-infection from the anterior vena cava into EDTA-containing tubes (Vacutainer) for total and differential white blood cell counts (performed using a Beckman Colter ACT, Beckman, Colter, CA) and quantification of viremia by virus titration as described above.

Peptides

Peptides representing the CSFV E2 FP (WT) and its derived mutants (mut-1 and mut-2, sequences displayed in Fig. 2A) were commercially synthesized (Thermo Scientific) and tagged with the 7-nitrobenz-2-oxa-l,3-diazole-4 (NBD) fluorophore at the N-terminus. The purified peptides were dissolved in dimethyl sulfoxide (DMSO, spectroscopy grade) and their concentrations determined by the bicinchoninic-acid microassay (Pierce, Rockford, IL, USA). Small, diluted aliquots (typically 20 μL, 1 mg/mL) were stored frozen and were thawed only once, upon use. 1-palmitoyl-2-oleoylphosphatidylglycerol (POPG) was purchased from Avanti Polar Lipids (Birmingham, AL). The 8-aminonaphthalene-1,3,6-trisulfonic acid sodium salt (ANTS) and p-xylenebis (pyridinium)bromide (DPX) were obtained from Molecular Probes (Junction City, OR). Dodecylphosphocholine (DPC) was from Anatrace (Maumee, OH, USA).

Circular dichroism srudies

Circular dichroism (CD) measurements were obtained from a thermally-controlled Jasco J-810 circular dichroism spectropolarimeter calibrated routinely with (1S)-(+)-10-camphorsulfonic acid, ammonium salt. Samples consisted of lyophilized peptides dissolved at concentrations of 0.03 mM in 2 mM Hepes (pH 7.4) buffer. Spectra were measured in a 1 mm pathlength quartz cell initially equilibrated at 25 °C. Data were taken with a 1 nm bandwidth at 100 nm/min speed, and the results of 20 scans were averaged.

Lipid monolayer penetration

Changes in surface pressure were monitored as a function of time in a fixed-area circular trough (μTrough S system, Kibron,

Helsinki) measuring 2 cm in diameter and with an aqueous volume of 1 ml (5 mM Hepes, 100 mM NaCl (pH 7.4)). Lipids, dissolved in chloroform, were spread over the surface and the desired initial surface pressure (π_0) was attained by changing the amount of lipid applied to the air-water interface. Peptides were injected into the subphase to a final concentration of 0.4 μM with a Hamilton microsyringe.

Lipid vesicle assays

Large unilamellar vesicles (LUV) made of POPG were prepared according to the extrusion method in 5 mM Hepes, 100 mM NaCl (pH 7.4) using membranes with a nominal pore-size of 0.1 μm. Partitioning into membranes was evaluated by monitoring the change in the emitted NBD-fluorescence. Corrected spectra were recorded using a FluoroMax-3 (Jobin Yvon Horiba, Longiumeau, France) with excitation set at 460 nm and 2-nm slits. Partitioning curves were subsequently computed from the fractional changes in emitted NBD-fluorescence when titrated with increasing lipid concentrations. The apparent mole fraction partition coefficients, $K_{x(app)}$, were determined by fitting the experimental values to a hyperbolic function:

$$F/F_0 = 1 + \frac{[(F_{max}/F_0) - 1][L]}{K + [L]} \quad (1)$$

where [L] is the lipid concentration and K is the lipid concentration at which the bound peptide fraction is 0.5. Therefore, $K_{x(app)} = [W]/K$ where [W] is the molar concentration of water.

tlsb-0.009w?>Vesicle permeabilization was assayed by monitoring the release to the medium of encapsulated fluorescent ANTS as described (Nieva et al., 1994). In brief, LUV containing 12.5 mM ANTS, 45 mM DPX, 20 mM NaCl and 5 mM Hepes were obtained by separating the unencapsulated material by gel-filtration in a Sephadex G-75 column that was eluted with 5 mM Hepes and 100 mM NaCl (pH 7.4). Fluorescence measurements were performed by setting the ANTS emission at 520 nm and the excitation at 355 nm. A cutoff filter (470 nm) was placed between the sample and the emission monochromator. The baseline leakage (0%) corresponded to the fluorescence of the vesicles at time 0, while 100% leakage was the fluorescence value obtained after addition of Triton X-100 (0.5% v/v).

Acknowledgments

This study was in part supported by Spanish MINECO and Basque Government grants (BIO2011-29792 and IT838-13 to J.L.N.). We thank the Plum Island Animal Disease Center animal care unit staff for excellent technical assistance. We specially thank Melanie Prarat for editing the manuscript.

References

Becher, P., Avalos Ramirez, R., Orlich, M., Cedillo Rosales, S., Konig, M., Schweizer, M., Stalder, H., Schirrmeier, H., Thiel, H.J., 2003. Genetic and antigenic characterization of novel pestivirus genotypes: implications for classification. Virology 311, 96–104.

Edwards, S., Moennig, V., Wensvoort, G., 1991. The development of an international reference panel of monoclonal antibodies for the differentiation of hog cholera virus from other pestiviruses. Vet. Microbiol. 29, 101–108.

El Omari, K., Iourin, O., Harlos, K., Grimes, J.M., Stuart, D.I., 2013. Structure of a pestivirus envelope glycoprotein E2 clarifies its role in cell entry. Cell Rep. 3, 30–35.

Gallaher, W.R., 1987. Detection of a fusion peptide sequence in the transmembrane protein of human immunodeficiency virus. Cell 50, 327–328.

Gallaher, W.R., 1996. Similar structural models of the transmembrane proteins of Ebola and avian sarcoma viruses. Cell 85, 477–478.

Gallaher, W.R., Ball, J.M., Garry, R.F., Griffin, M.C., Montelaro, R.C., 1989. A general model for the transmembrane proteins of HIV and other retroviruses. AIDS Res. Hum. Retrovir. 5, 431–440.

Gallaher, W.R., DiSimone, C., Buchmeier, M.J., 2001. The viral transmembrane superfamily: possible divergence of Arenavirus and Filovirus glycoproteins from a common RNA virus ancestor. BMC Microbiol. 1, 1.

Garry, R.F., Dash, S., 2003. Proteomics computational analyses suggest that hepatitis C virus E1 and pestivirus E2 envelope glycoproteins are truncated class II fusion proteins. Virology 307, 255–265.

Gregory, S.M., Harada, E., Liang, B., Delos, S.E., White, J.M., Tamm, L.K., 2011. Structure and function of the complete internal fusion loop from Ebolavirus glycoprotein 2. Proc. Natl. Acad. Sci. U.S.A 108, 11211–11216.

Hulst, M.M., Moormann, R.J., 1997. Inhibition of pestivirus infection in cell culture by envelope proteins E(rns) and E2 of classical swine fever virus: E(rns) and E2 interact with different receptors. J. Gen. Virol. 78 (11), 2779–2787.

Iourin, O., Harlos, K., El Omari, K., Lu, W., Kadlec, J., Iqbal, M., Meier, C., Palmer, A., Jones, I., Thomas, C., Brownlie, J., Grimes, J.M., Stuart, D.I., 2013. Expression, purification and crystallization of the ectodomain of the envelope glycoprotein E2 from Bovine viral diarrhoea virus. Acta crystallographica. Section F. Struct. Biol. Cryst. Commun. 69, 35–38.

Kuhn, R.J., Zhang, W., Rossmann, M.G., Pletnev, S.V., Corver, J., Lenches, E., Jones, C.T., Mukhopadhyay, S., Chipman, P.R., Strauss, E.G., Baker, T.S., Strauss, J.H., 2002. Structure of dengue virus: implications for flavivirus organization, maturation, and fusion. Cell 108, 717–725.

Langedijk, J.P., 2002. Translocation activity of C-terminal domain of pestivirus Erns and ribotoxin L3 loop. J Biol. Chem. 277, 5308–5314.

Largo, E., Gladue, D.P., Huarte, N., Borca, M.V., Nieva, J.L., 2014. Pore-forming activity of pestivirus p7 in a minimal model system supports genus-specific viroporin function. Antiviral research 101, 30–36.

Lescar, J., Roussel, A., Wien, M.W., Navaza, J., Fuller, S.D., Wengler, G., Wengler, G., Rey, F.A., 2001. The fusion glycoprotein shell of Semliki forest virus: an icosahedral assembly primed for fusogenic activation at endosomal pH. Cell 105, 137–148.

Li, Y., Wang, J., Kanai, R., Modis, Y., 2013. Crystal structure of glycoprotein E2 from bovine viral diarrhea virus. Proc. Natl. Acad. Sci. U.S.A 110, 6805–6810.

Liang, D., Sainz, I.F., Ansari, I.H., Gil, L.H., Vassilev, V., Donis, R.O., 2003. The envelope glycoprotein E2 is a determinant of cell culture tropism in ruminant pestiviruses. J. Gen. Virol. 84, 1269–1274.

Marsh, D., 2007. Lateral pressure profile, spontaneous curvature frustration, and the incorporation and conformation of proteins in membranes. Biophys. J. 93, 3884–3899.

Mittelholzer, C., Moser, C., Tratschin, J.D., Hofmann, M.A., 2000. Analysis of classical swine fever virus replication kinetics allows differentiation of highly virulent from avirulent strains. Vet. Microbiol. 74, 293–308.

Nieva, J.L., Agirre, A., 2003. Are fusion peptides a good model to study viral cell fusion? Biochim. Biophys. Acta 1614, 104–115.

Nieva, J.L., Nir, S., Muga, A., Goni, F.M., Wilschut, J., 1994. Interaction of the HIV-1 fusion peptide with phospholipid vesicles: different structural requirements for fusion and leakage. Biochemistry 33, 3201–3209.

Rafalski, M., Lear, J.D., DeGrado, W.F., 1990. Phospholipid interactions of synthetic peptides representing the N-terminus of HIV gp41. Biochemistry 29, 7917–7922.

Reed, L.J., Muench, H.A., 1938. A simple method of estimating fifty per cent endpoints. Am. J. Trop. Med. Hyg. 27, 493–497.

Rey, F.A., Heinz, F.X., Mandl, C., Kunz, C., Harrison, S.C., 1995. The envelope glycoprotein from tick-borne encephalitis virus at 2 A resolution. Nature 375, 291–298.

Rice, C.M., 1996. Flaviviridae: the viruses and their replication. In: Fields, B.N., Knipe, D.M., Howley, P.M. (Eds.), Fundamental Virology, 3rd ed. Lippincott, Raven, Philadelphia, pp. 931–959

Risatti, G.R., Borca, M.V., Kutish, G.F., Lu, Z., Holinka, L.G., French, R.A., Tulman, E.R., Rock, D.L., 2005. The E2 glycoprotein of classical swine fever virus is a virulence determinant in swine. J. Virol. 79, 3787–3796.

Risatti, G.R., Holinka, L.G., Carrillo, C., Kutish, G.F., Lu, Z., Tulman, E.R., Sainz, I.F., Borca, M. V., 2006. Identification of a novel virulence determinant within the E2 structural glycoprotein of classical swine fever virus. Virology 355, 94–101.

Risatti, G.R., Holinka, L.G., Fernandez Sainz, I., Carrillo, C., Kutish, G.F., Lu, Z., Zhu, J., Rock, D.L., Borca, M.V., 2007a. Mutations in the carboxyl terminal region of E2 glycoprotein of classical swine fever virus are responsible for viral attenuation in swine. Virology 364, 371–382.

Risatti, G.R., Holinka, L.G., Fernandez Sainz, I., Carrillo, C., Lu, Z., Borca, M.V., 2007b. N-linked glycosylation status of classical swine fever virus strain Brescia E2 glycoprotein influences virulence in swine. J. Virol. 81, 924–933.

Sanger, F., Nicklen, S., Coulson, A.R., 1977. DNA sequencing with chain-terminating inhibitors. Proc. Natl. Acad. Sci. U.S.A 74, 5463–5467.

Thiel, H.J., Stark, R., Weiland, E., Rumenapf, T., Meyers, G., 1991. Hog cholera virus: molecular composition of virions from a pestivirus. J. Virol. 65, 4705–4712.

van Gennip, H.G., Bouma, A., van Rijn, P.A., Widjojoatmodjo, M.N., Moormann, R.J., 2002. Experimental non-transmissible marker vaccines for classical swine fever (CSF) by trans-complementation of E(rns) or E2 of CSFV. Vaccine 20, 1544–1556.

van Gennip, H.G., van Rijn, P.A., Widjojoatmodjo, M.N., de Smit, A.J., Moormann, R.J., 2000. Chimeric classical swine fever viruses containing envelope protein E (RNS) or E2 of bovine viral diarrhoea virus protect pigs against challenge with CSFV and induce a distinguishable antibody response. Vaccine 19, 447–459.

Van Gennip, H.G., Vlot, A.C., Hulst, M.M., De Smit, A.J., Moormann, R.J., 2004. Determinants of virulence of classical swine fever virus strain Brescia. J. Virol. 78, 8812–8823.
Wang, Z., Nie, Y., Wang, P., Ding, M., Deng, H., 2004. Characterization of classical swine fever virus entry by using pseudotyped viruses: E1 and E2 are sufficient to mediate viral entry. Virology 330, 332–341.
Weiland, E., Stark, R., Haas, B., Rumenapf, T., Meyers, G., Thiel, H.J., 1990. Pestivirus glycoprotein which induces neutralizing antibodies forms part of a disulfide-linked heterodimer. J. Virol. 64, 3563–3569.
Weiland, F., Weiland, E., Unger, G., Saalmuller, A., Thiel, H.J., 1999. Localization of pestiviral envelope proteins E(rns) and E2 at the cell surface and on isolated particles. J. Gen. Virol. 80 (5), 1157–1165.
Zsak, L., Lu, Z., Kutish, G.F., Neilan, J.G., Rock, D.L., 1996. An African swine fever virus virulence-associated gene NL-S with similarity to the herpes simplex virus ICP34.5 gene. J. Virol. 70, 8865–8871.